Development 125, 2125-2134 (1998)
Printed in Great Britain © The Company of Biologists Limited 1998
DEV6325

Drosophila β_{Heavy}-spectrin is essential for development and contributes to specific cell fates in the eye

Graham H. Thomas[1,‡], Daniela C. Zarnescu[1], Amy E. Juedes[1,*], Mark A. Bales[1,†], Amy Londergan[1], Carol C. Korte[1] and Daniel P. Kiehart[2]

[1]Departments of Biology and of Biochemistry and Molecular Biology, The Pennsylvania State University, University Park, PA 16802, USA
[2]Department of Cell Biology, Duke University Medical Center, Durham, NC 27710, USA
*Present address: Section of Immunobiology, Yale University School of Medicine, 330 Cedar Street, P.O. Box 208011, New Haven, CT 06520, USA
†Present address: Department of Cell Biology and Anatomy, University of Arizona, College of Medicine, Tucson, AZ 85724, USA
‡Author for correspondence (e-mail: GXT5@PSU.EDU)

Accepted 31 March; published on WWW 6 May 1998

SUMMARY

The spectrin membrane skeleton is a ubiquitous cytoskeletal structure with several cellular roles, including the maintenance of cell integrity, determination of cell shape and as a contributor to cell polarity. We have isolated mutations in the gene encoding β_{Heavy}-spectrin in *Drosophila*, and have named this essential locus *karst. karst* mutant individuals have a pleiotropic phenotype characterized by extensive larval lethality and, in adult escapers, rough eyes, bent wings, tracheal defects and infertility. Within *karst* mutant eyes, a significant number of ommatidia specifically lack photoreceptor R7 alongside more complex morphological defects.

Immunolocalization of β_{Heavy}-spectrin in wild-type eye-antennal and wing imaginal discs reveals that β_{Heavy}-spectrin is present in a restricted subdomain of the membrane skeleton that colocalizes with *D*E-cadherin. We propose a model where normal levels of Sevenless signaling are dependent on tight cell-cell adhesion facilitated by the β_{Heavy}-spectrin membrane skeleton.

Immunolocalization of β_{Heavy}-spectrin in the adult and larval midgut indicates that it is a terminal web protein, but we see no gross morphological defects in the adult apical brush border in *karst* mutant flies. Rhodamine phalloidin staining of *karst* mutant ovaries similarly reveals no conspicuous defect in the actin cytoskeleton or cellular morphology in egg chambers. This is in contrast to mutations in α-spectrin, the molecular partner of β_{Heavy}-spectrin, which affect cellular structure in both the larval gut and adult ovaries.

Our results emphasize the fundamental contribution of the spectrin membrane skeleton to normal development and reveals a critical interplay between the integrity of a cell's membrane skeleton, the structure of cell-cell contacts and cell signaling.

Key words: Spectrin, Cell adhesion, Cell signaling, *Drosophila*, Eye

INTRODUCTION

The spectrin-based membrane skeleton is a ubiquitous cellular structure that plays a role in the maintenance of cell shape and cell integrity, the generation and/or maintenance of cell polarity and formation of cell adhesion complexes (Bennett and Gilligan, 1993; Drubin and Nelson, 1996). Mutations in the membrane skeleton components of human erythrocytes result in haemolytic anaemias (Becker and Lux, 1995). In non-erythroid tissues, localized subcellular differentiation of the membrane skeleton facilitates cell polarity either by creating targeting patches to which proteins are recruited, or by the specific retention of delivered proteins (reviewed in Drubin and Nelson, 1996; Nelson, 1992). The utilization of different spectrin isoforms, generated by alternative splicing and the combinatorial association of α and β chains (Bennett and Gilligan, 1993; Luna and Hitt, 1992), is likely to be a key step in creating such biochemically distinct membrane domains. Supporting this hypothesis, different spectrins have differing subcellular distributions (Lazarides et al., 1984; Riederer et al., 1986; Lambert and Bennett, 1993). Genetic analysis of the functions of the non-erythroid membrane skeleton are just beginning to bear fruit.

In *Drosophila* several components of this membrane skeleton have been identified. These include both α-spectrin and β-spectrin (Byers et al., 1992; Dubreuil et al., 1989), β_{Heavy}-spectrin (Dubreuil et al., 1990; Thomas and Kiehart, 1994; Thomas et al., 1997), protein 4.1 isoforms (Boedigheimer et al., 1993; Fehon et al., 1993), adducin-like proteins (Yue and Spradling, 1992; Ding et al., 1993; Zaccai and Lipshitz, 1996) and ankyrin (Dubreuil and Yu, 1994). Mutations in several of these genes indicate that the membrane skeleton is essential for development, but have not yet revealed the molecular mechanism by which they interfere with development.

The combinatorial association of *Drosophila* spectrin monomers produces either α_2/β_2 or α_2/β_{H2} tetramers (Dubreuil et al., 1990). Both tetramers crosslink actin and contain β-chain PH and α-chain SH3 domains (Byers et al., 1992; Dubreuil et al., 1989, 1990; Thomas et al., 1997; Musacchio et al., 1993, 1994), supporting the notion that spectrins interact with several cellular components other than actin. β_H, with 30 spectrin repeats and a $M_r = 470\times10^3$, is longer and more massive than conventional β-spectrins (~250×10^3 M_r, 17 repeats). β_H is also unique among β-isoforms in containing an SH3 domain and in that it probably does not bind to ankyrin (Thomas et al., 1997). Although β_H was first recognized in the fly, it is of ancient origin (Thomas et al., 1997), has recently been cloned from *Caenorhabditis elegans* (McKeown et al., 1998) and may have a vertebrate homologue in the TW260/240 β-chain (Glenney et al., 1983). In polarized epithelia, α-spectrin is generally distributed on plasma membranes (Lee et al., 1993; Pesacreta et al., 1989; this paper), while β-spectrin is restricted to the basolateral surface (de Cuevas et al., 1996; Lee et al., 1993, 1997), and β_H is localized to the apical domain at the adherens junction, on the free apical surface and under brush borders (Thomas and Kiehart, 1994; Wodarz et al., 1995; Uemura et al., 1996; de Cuevas et al., 1996; Lee et al., 1997; this paper). Recruitment of β-spectrin to the membrane can occur after adhesion events in fly (Dubreuil et al., 1996) and vertebrate tissue culture cells (Drubin and Nelson, 1996). However, during early development in *Drosophila* the β_H membrane skeleton becomes polarized prior to formation of mature adherens junctions (Müller and Wieschaus, 1996; Tepass and Hartenstein, 1994; Thomas and Kiehart, 1994). This suggests the hypothesis that different β isoforms may be recruited in different ways.

Although both α-spectrin and β-spectrin have been shown to be essential (Lee et al., 1993; Deng et al., 1995; Lee et al., 1996, 1997; de Cuevas et al., 1996), little is still known about the precise role of spectrin in the non-erythroid membrane skeleton during development. To further elucidate these roles, we have generated mutations in the gene encoding the apical β-spectrin, β_H. We have named this new locus *karst* (abbr. *kst*), for the resemblance of the rough eye phenotype to certain karst landforms where domed hills are separated by flat valleys. We show that this gene is essential for the normal development of adult epithelial structures and for the production of photoreceptor R7 in the eye-antennal imaginal disc. We show that β_H is polarized in imaginal disc epithelia and is present in the terminal web of intestinal cells. Furthermore, we demonstrate tight colocalization of β_H and *D*E-cadherin in imaginal discs, and show that both proteins exhibit elevated staining in developing ommatidial preclusters in the eye disc. Our data suggest the hypothesis that high fidelity Sevenless signaling is dependent on the cytoskeleton at the adherens junction. These results illustrate how the correct integration of cell structure, adhesion and signaling is necessary for normal development. The data presented complement the recent description of mutations in the homologous protein in *Caenorhabditis elegans* (McKeown et al., 1998).

MATERIALS AND METHODS

Fly stocks

Deficiencies used were *Df(3L)HR277*, *Df(3L)HR232*, *Df(3L)HR119*, *Df(3L)1226* and *Df(3L)663*, and removed 63B6-64B12, 63C1-63D3, 63C6-E9, 63C6-E1 and 63D3-E1, respectively (Wohlwill and Bonner, 1991; Paine-Saunders, 1989). The mutation *l(3)B1-14.1* proved to be an allele of *karst* and is now designated $kst^{B1\text{-}14.1}$ (Paine-Saunders, 1989). The latter three mutations were induced on the *mwh red e* chromosome. The progenitor strain for our mutagenesis was *mwh ve red*. A P-element insertion into *karst* was identified in the Berkeley Drosophila Genome Project collection (Karpen and Spradling, 1992). This insert $P\{PZ\}l(3)01318^{01318}$ is now designated $P\{PZ\}karst^{01318}$ (abbr. kst^{01318} in this paper).

Mutagenesis

Suitable deficiencies for mutagenesis were screened for deletion of the β_H coding sequences by quantitative Southern blot. DNA extracted by standard procedures (Ashburner, 1989) from the deficiency stocks was digested with *Bam*HI and *Eco*RI, run on a gel and blotted. The blot was simultaneously probed with a ~1 kb β_H fragment (nt 3761-4936 of pBH5; Dubreuil et al., 1990) that was co-labeled with the insert of p88.3 which contains the *hsp26* gene (Corces et al., 1980) as an undeleted reference. The large deficiency *Df(3L)HR277* that cytologically removed the region encompassing the β_H gene, based on in situ hybridization data (Dubreuil et al., 1990), confirmed the validity of this approach.

Mutagenesis followed standard procedures for an F_2 lethal screen (Grigliatti, 1986) using ethane methane sulphonate at 31 mM as a mutagen. Mutagenized chromosomes were screened for lethality over *Df(3L)1226* and counter screened for non-lethality over *Df(3L)663*, which does not remove the β_H gene but is contained within the region uncovered by *Df(3L)1226*.

The site of the P-element insertion in $P\{PZ\}kst^{01318}$ was identified as follows. PCR between a primer specific for the end of the P element (Ballinger and Benzer, 1989) and each of the two primers RCSEQ1 (5′-TAGTATCCTGGCGCACA-3′) and RCPRIM1 (5′-AGCGGGC-CAATAAGTAAA-3′) on either side of the P element mapped the insertion site to near the 3′ end of the first intron in *karst*. Direct sequencing of these purified PCR fragment pools following gel purification refined this location to between positions 662 and 663 of intron 1 and identified an accompanying 8 bp duplication of the neighbouring intron sequence (data not shown). We have remobilized the P{PZ} transposon in this allele (confirmed by sequencing) and have demonstrated that *ry* revertants fully complement kst^1, kst^2 and *Df(3L)1226* (other alleles were not tested).

Antibodies and immunoblots

β_H was identified on immunoblots with serum #243, which is directed against the N-terminal 144 kD of β_H (Thomas and Kiehart, 1994) used at a dilution of 1/1500. For immunofluorescent localization of β_H in fixed tissues, polyclonal anti-β_H antibodies were affinity purified from rabbit serum 243 as previously described (Thomas and Kiehart, 1994) and used at a dilution of 1/10. In some specimens, an anti-β_H monoclonal antibody (mAb 5.73) was used at a dilution of 1/2 from the culture supernatant. This antibody was derived from a mouse for which the polyclonal serum has been previously described (Thomas and Kiehart, 1994). α-spectrin was immunolocalized using rabbit antiserum #905 at a concentration of 1/500 (Byers et al., 1987). *D*E-cadherin was immunolocalized using the mAb DCAD2 (Oda et al., 1994) at a concentration of 1/10. The secondary antibody for immunoblotting was alkaline phosphatase-conjugated goat anti-rabbit antibody (Promega, Madison, WI) used at 1/2000. For immunolocalizations an affinity-purified FITC-conjugated goat anti-mouse, or Cy3-conjugated goat anti-rabbit antibody was used (Jackson Immunoresearch Laboratories Inc., West Grove, PA). Immunoblots were done as previously described (Thomas and Kiehart, 1994), except that flies and larvae were ground in the 2× loading buffer at room temperature and the secondary antibody (Promega, Madison, WI) was used as described above.

Immunolocalization of proteins

Optimal fixation of imaginal disc tissue for staining with spectrin antibodies used a fixation method combining methanol and PLP (75 mM lysine, 2% paraformaldehyde, 0.01 M $NaIO_4$, 37 mM sodium phosphate buffer, pH 7.4; McLean and Nakane, 1974) as follows. Tissues were dissected in 100 mM sodium phosphate buffer, pH 7.2, at room temperature, accumulated in buffer on ice and fixed in 100% methanol on ice for 10 minutes. Samples were then rehydrated through a methanol:PLP series (70:30%, 50:50%, 30:70%) for 5 minutes each on ice, followed by two incubations in PLP alone for 10 minutes each. Optimal fixation for *D*E-cadherin used only PLP for a total of 45 minutes on ice. Fixed eye-imaginal discs were washed three times in dissection buffer (0.1% saponin, 100 mM sodium phosphate buffer, pH 7.2), during which the peripodial membrane was dissected away. Subsequent blocking, primary and secondary antibody incubations, and washes were all performed in blocking solution (0.1% saponin, 10% normal goat serum [NGS], 100 mM sodium phosphate buffer, pH 7.2). Discs were blocked for 15-20 minutes and incubated with the primary antibody for 3 hours at room temperature. Following two 10 minute washes, the discs were incubated for 2 hours in the appropriate secondary antibody. Wing discs were subjected to a similar treatment except that the peripodial membrane was not removed and saponin was used at a concentration of 0.2%.

β_H is not well preserved without the methanol fixation, while *D*E-cadherin is disrupted by this treatment. Thus, in order to demonstrate colocalization of β_H with DE-cadherin, we used a compromise fixation that preserves antigenicity of both β_H and *D*E-cadherin, but only reliably in the more prominent type III adherens junctions in the eye disc (Takahashi et al., 1996). This procedure is based on that of Bell and Safiejko-Mroczka (1995). Discs were dissected in *Drosophila* Ringers (Ashburner, 1989), and then incubated for 15 minutes at room temperature in Ringers plus 40 μg/ml dithiobis(succinimidylpropionate) (DSP; Pierce, Rockford IL). The DSP solution was prepared by diluting a 20 mg/ml stock in DMSO 1/500 in Ringers. Discs were then fixed in PLP for 30 minutes at room temperature, washed twice for 10 minutes each in BSS (38 mM NaCl, 53 mM KCl, 12 mM $MgSO_4$, 0.5 mM $CaCl_2$, 1 mM tricine, 2 mM glucose, 5 mM sucrose, 0.2% bovine serum albumin adjusted to pH 7; Van Vactor et al., 1991) and incubated with the primary antibody in BSN (BSS plus 3% NGS; Van Vactor et al., 1991). Subsequent washes and secondary antibody incubations used BSS and BSN, respectively, using similar times and temperatures to the single staining protocols. All samples were equilibrated in mounting medium (80% glycerol, 2% propyl gallate, 100 mM Tris-HCl, pH 8.5) prior to examination to counteract photobleaching.

To immunolocalize β_H in the adult midgut, flies were dissected in *Drosophila* Ringers (Ashburner, 1989) and fixed in Ringers plus 1% glutaraldehyde for 10 minutes at room temperature. The guts were rinsed 3 times in PBS (130 mM NaCl, 7 mM Na_2HPO_4, 3 mM NaH_2PO_4, pH 7.0) plus 0.1% Triton X-100 (PBT), blocked in PBT plus 10% normal goat serum for 1 hour and incubated with affinity-purified 243 serum diluted 1/10 in blocking solution overnight at 4°C. The guts were washed 4 times in PBT and the primary antibody localized with the Vectastain kit (Vector Laboratories Inc., Burlingame, CA) according to the manufacturers instructions, dehydrated through an ethanol series, embedded in paraffin wax and sectioned. After removal of the wax with xylene, sections were permanently embedded using Permount (Sigma Chemicals, St Louis, MO).

Samples were imaged as previously described (Kiehart et al., 1994) with slight modifications. Briefly, for immunofluorescence we used a cooled Dage-MTI CCD72T camera (Dage-MTI Inc., Michigan City, IN) mounted on an Olympus BX50 microscope equipped for immunofluorescence (Olympus America Inc., Lake Success, NY). Image capture was via a Data Translation DT 2255 frame grabber (Data Translation, Marlboro, MA) mounted in an Macintosh 8100/80AV computer (Apple Computer, Cupertino, CA) and controlled by the public domain program NIH Image (v1.55, available on the internet at http://rsb.info.nih.gov/nih-image/) for immunofluorescence and ColorKit (Data Translation, Marlboro, MA) for DAB precipitates. Post-capture processing used NIH Image and/or Adobe Photoshop v2.5 or v4.0 (Adobe Systems, San Jose, CA) and composites were prepared and annotated using Canvas v3.5 (Deneba Software, Miami, FL) or Adobe Illustrator v6.0.

RESULTS

Isolation of *karst* mutant alleles

Mutations in the locus encoding β_{Heavy}-spectrin (β_H) were recovered in standard screens. The location of the β_H gene, previously assigned to the cytological interval 63C1-D3 (Dubreuil et al., 1990), was refined by quantitative Southern blots of DNA extracted from stocks carrying deficiencies in this region (see Materials and Methods), narrowing the location to the region uncovered by *Df(3L)1226* but not *Df(3L)663* (63C6-D2). Using *Df(3L)1226* for our mutagenesis (see Materials and Methods), we isolated 26 lethal and semilethal lines from ~3800 mutagenized chromosomes analyzed. All mutant lines were screened by immunoblot for β_H protein abnormalities using antiserum #243 (Thomas and Kiehart, 1994). One complementation group, represented by two alleles, affected the β_H protein. We have named this locus *karst*, and the two alleles produce either a truncated β_H product ~200×10^3 M_r (*kst*^{1}; Fig. 1) or no detectable β_H (*kst*^{2}; Fig. 1) using serum #243. Subsequent complementation tests with pre-existing mutations in the region identified *l(3)B1-14.1* (Paine-Saunders, 1989) to be an allele of *karst* (now designated *kst*$^{B1\text{-}14.1}$). *kst*$^{B1\text{-}14.1}$ produces no detectable protein (data not shown). We have also

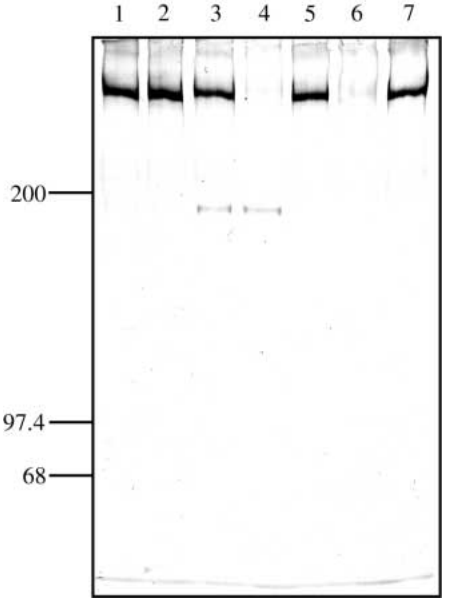

Fig. 1. The *karst* mutation affects β_H protein. Immunoblot of whole fly extracts probed for β_H with the polyclonal antiserum #243 (Materials and Methods). The genotypes of the flies analyzed are: (1) *mwh ve red* (progenitor stock); (2) *mwh Df(3L)1226 red e/* TM6, *Tb Hu e*; (3) *mwh ve kst*^{1} *red* /TM6, *Tb Hu e*; (4) *mwh ve kst*^{1} *red* /*mwh Df(3L)1226 red e;* (5) *mwh ve kst*$^{2\ red}$ /TM6, *Tb Hu e*; (6) *mwh ve kst*^{2} *red* /*mwh Df(3L)1226 red e*; and (7) same as lane 1.

identified an allele (*kst*^{01318}) resulting from a P-element insertion into the first intron of the *karst* gene within the 5′ untranslated region. This allele produces apparently full-length β_H protein (by immunoblot; data not shown), is much more viable than the other *karst* alleles, but fails to compliment the rough eye phenotype of all tested *karst* alleles. Given the site of insertion, the abundant protein in whole fly extracts and the observation that only the eye phenotype is penetrant (see below), suggests that this allele affects a regulatory site necessary for tissue-specific expression or mRNA processing. Excision of this P element abolishes the *karst* eye phenotype associated with this allele, so we conclude that the *karst*^{01318} phenotype is wholly due to the presence of the P{PZ} element.

The evidence that the *karst* locus encodes β_H is as follows: (1) three alleles exhibit a β_H protein abnormality; (2) the alleles form a complementation group and fully complement the other lethal mutations uncovered by *Df(3L)1226*; (3) *kst*$^{B1\text{-}14.1}$ and *kst*^{01318} were generated in independent mutageneses on different progenitor chromosomes (Karpen and Spradling, 1992; Paine-Saunders, 1989); (4) no gross DNA abnormalities are detectable in the ~42 kb of genomic DNA encompassing the β_H-coding region of the *kst*^{1} and *kst*^{2} alleles (data not shown), so the lesions generated are small and probably do not affect adjacent genes; (5) the P element in *kst*^{01318} is physically located in the first intron of the gene and its excision eliminates the *karst* phenotype arising from this allele and (6) all combinations of *karst* mutant alleles over one-another and over deficiencies have comparable phenotypes (with the exception of *kst*^{01318}; see above), suggesting that they all result in a similar loss-of-function phenotype. Together, these six lines of evidence demonstrate that the phenotype described in this paper arises from mutations in the *karst* gene. Furthermore, to eliminate the effects of ancillary mutations all of our experiments are done in heterozygous allelic combinations or over deficiencies. While, in principle, it would be useful to rescue the *karst* mutation with a transposon-based construct, the huge size of this transcript (~13 kb) means that this has been unsuccessful to date.

Table 1. Variable viability in inter se crosses with *karst* mutants

	kst^{2}	*kst*$^{B1\text{-}14.1}$	*Df(3L)1226*	*Df(3L)HR232*
kst^{1}	2.1±1.3 (5x, 3216)	13±4.6 (4x, 1252)	3.8±3.6 (12x, 4795)	11.6±3.6 (8x, 2140)
kst^{2}	*	12.1±5.8 (4x, 2558)	4.0±5.3 (4x, 2428)	11.7±3.8 (4x, 1905)
kst$^{B1\text{-}14.1}$		*	0.7 (2x, 886)	12.9 (2x, 961)

The table indicates the percentage of *karst* mutant individuals recovered with 25% being the Mendelian expectation for this class. (nx, #) n crosses scored, and the total number of individuals scored to derive the viability of each mutant class. Note the large standard deviations illustrating the great variability around these averages despite several repetitions and large numbers of individuals scored.

*These numbers cannot be obtained at present due to the presence of ancillary lethals.

karst mutant phenotypes

The *karst* mutant phenotype is semilethal and poorly fertile. Thus, *karst* stocks cannot be maintained in the homozygous mutant state. All *karst* mutant embryos hatch; but, *karst* mutant pupae are present at less than 10% of Mendelian expectation suggesting that most individuals die as larvae. Indeed, washing and filtration of larvae from the food reveals carcasses of all instars. There seems to be little if any pupal lethality and *karst* mutants eclose 2-4 days behind their wild-type siblings. The frequency at which *karst* mutants eclose thus indicates the proportion of individuals that die as larvae and is very variable (Table 1). This variation does not appear to be a function of the sex of the parent, culture density, temperature or type of food. The most extreme allelic combinations produce few or no adults.

Adult escapers have a complex visible phenotype exhibiting variable expressivity and/or penetrance. In descending order of penetrance *karst* mutant flies possess rough eyes (Fig. 2B,C), wings that typically curve downwards in an ‘inverted spoon’

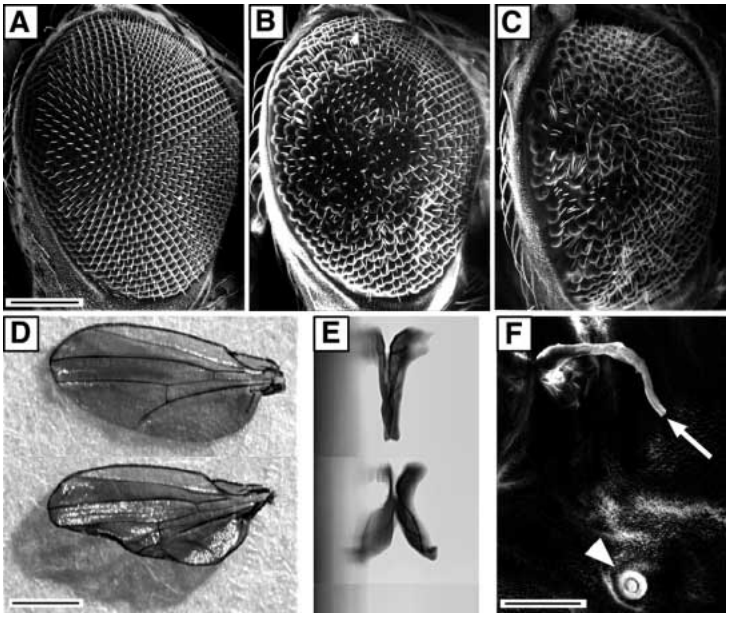

Fig. 2. The visible *karst* phenotype reveals defects in tissues of epithelial origin. (A) Wild-type eye (*mwh ve red*); (B,C) examples of the *karst* rough eye phenotype (B is *mwh ve kst*^{1}*/mwh Df(3L)1226 red e*; C is *mwh ve kst* ^{1}*red / mwh ve kst*^{2} *red*); (D,E) comparison of a wild type (upper) and *karst* mutant wing (lower; genotype – *mwh ve kst* ^{1}*red/ mwh ve kst*^{2} *red*). (D) Ventral view with oblique lighting; (E) end-on view with the distal tip closest to camera, apical to the left. The wild-type wing is essentially planar (hinge region is slightly bent towards the ventral side) while the *karst* mutant wing curves gently downwards; (F) scanning electron micrograph of two abdominal spiracles on a *karst* mutant individual (*mwh ve kst*^{1}*/mwh Df(3L)1226 red e*). Anterior is down, dorsal is to the left; The spiracle in segment A2 contains a plug of material (arrowhead) and melanized material has been extruded from the spiracle in A3 (arrow). Scale bars: in A (for A-C) is 100 μm; in D (for D,E) is 500 μm; in F is 50 μm.

shape (Fig. 2D,E) and visible extrusion of material from the abdominal spiracles (Fig. 2F). These melanized protrusions appear most commonly in (but are not restricted to) abdominal segment 3 and usually several spiracles can be seen to have material within them. We presume this is coagulated haemolymph and reflects a loss of tracheal integrity. *karst* mutant escapers are very infertile and produce low numbers of eggs. It is unlikely that the *karst* mutation has a large effect on cell proliferation or viability in imaginal tissues, since neither the wings nor the eyes appear reduced in size. Immunoblots of *karst* mutant larvae indicate that, by the third instar, it is no longer possible to detect maternally contributed β_H (data not shown), so these phenotypes represent metamorphosis in the absence of detectable wild-type product. Below we present an initial analysis of the *karst* eye phenotype and relate this to the distribution of β_H in imaginal tissues.

The *karst* eye phenotype

karst mutant eyes appear roughest towards the posterior margin where ommatidia are sometimes absent (Figs 2B,C, 3C). Although the phenotype of the most severe *karst* mutant eyes resembles that of the EGF receptor mutation $DER^{Ellipse}$ (Baker and Rubin, 1992), we have observed no dominant interaction between these loci (H. Rizkalla and G. H. T., unpublished observations). *karst* mutant eyes also exhibit a variable frequency of ommatidia that are lacking photoreceptor R7 (up to 61%; Table 2). We have confirmed that it is R7 that is absent by examining serial sections through *karst* mutant eyes. Ommatidia with only six photoreceptors in distal sections (relative to the brain) had seven in proximal sections (Fig. 3D,E). Since R1-6 extend the entire depth of the retina while R7 extends only through distal regions and R8 replaces R7 in more proximal regions, this result is consistent with the specific absence of R7. At a lower frequency *karst* mutant eyes also contain ommatidia with very abnormal numbers of photoreceptors. The morphology of such clusters suggests that they may have arisen through fusion of ommatidia to another cluster containing only a small number of photoreceptors. Finally, some photoreceptors have greatly expanded rhabdomeres (Fig. 3F-I). Serial sectioning reveals that these are broader throughout the depth of the retina and do not result from a failure of such cells to extend properly during pupation. The roughening of the eye is 100% penetrant but exhibits variable expressivity.

Table 2. Frequency of photoreceptor abnormalities in *karst* mutants

	kst1/Df(3L)HR232	kst2/Df(3L)1226	kst1/kst2
8R	45.7±43.5	68.0±36.4	33.9±28.7
7R	53.9±43.2	24.4±30.3	61.4±30.8
#R	0.4±0.9	5.7±6.3	1.5±2.8
Fusions	0	2.0±2.4	3.2±4.1

Sections of *karst* mutant eyes were scored for photoreceptor number and likely cluster fusions. 8R, eight photoreceptors; 7R, ommatidia lacking R7; #R, other numbers of photoreceptors; Fusions, clusters whose morphology is suggestive of ommatidial fusion due to their arrangement in two or more groupings with the absence of intervening pigment cells. Mean percentages of at least 4 eyes and a total of 300 ommatidia are shown ± 1 s.d. Note that these aspects of the phenotype also show considerable variation in expressivity.

Within ommatidia that do have eight photoreceptors, the arrangement of these cells is not as regular as in wild-type eyes (Fig. 3B-D). However, the presence of a recognizable trapezoid in many ommatidia indicates that this patterning event is intact in *karst* mutants and reveals an equatorial line, so cluster rotation still occurs. To try and place β_H in the

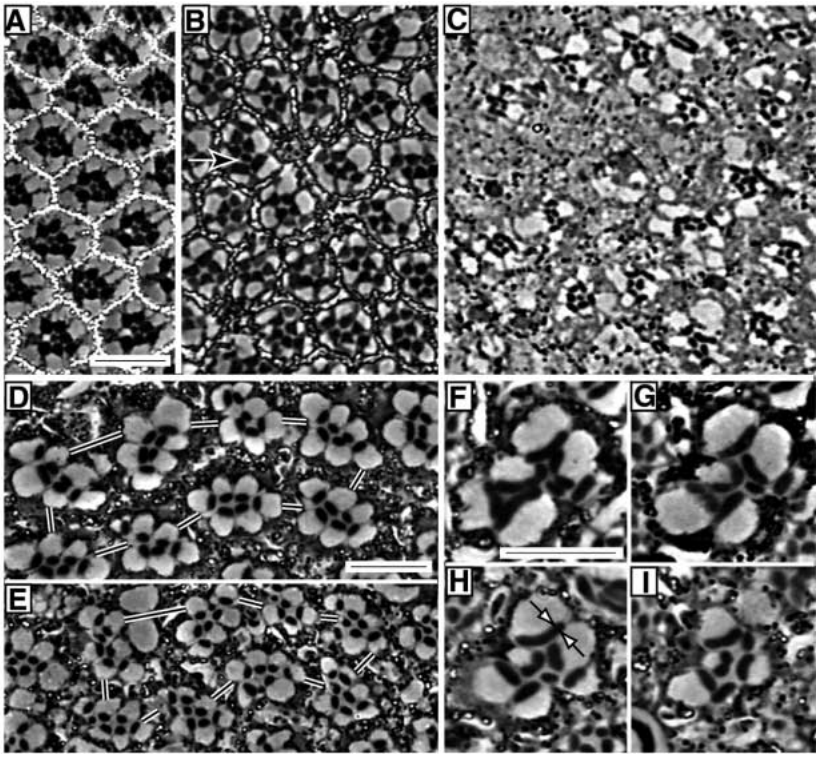

Fig. 3. Sections of *karst* mutant eyes reveal aberrant tissue architecture and a sevenless phenotype. (A) The progenitor strain, *mwh ve red*; (B) a mild *karst* mutant eye (*mwh ve kst[1] red/Df(3L)HR232)*. Note the absence of the small inner R7 photoreceptor in all but one ommatidium in this panel (arrow) and the generally poor morphology. (C) A severe *karst* mutant eye missing many ommatidia (*mwh ve kst[1] red/Df(3L)1226*). (D,E) Serial sectioning reveals that ommatidia showing only 6 photoreceptors approximately 34 μm below the lens (D), infact have 7 approximately 60 μm below the lens in the region of R8 (E). This is consistent with the specific absence of R7 in these ommatidia. The equivalent group of 8 ommatidia in each section are linked by lines (*mwh ve kst[1] red/mwh ve kst[2] red*). (F-I) Four sections from a serial group through a cluster exhibiting the extended rhabdomere morphology. Such clusters are usually grossly disorganized. Note that while the apical domain is expanded, the length of the microvilli appears to remain similar to wild type (opposing arrows). This is the same eye as in D and E. Scale bars in A (for A-C), D (for D,E) and F (for F-I) all represent 10 μm.

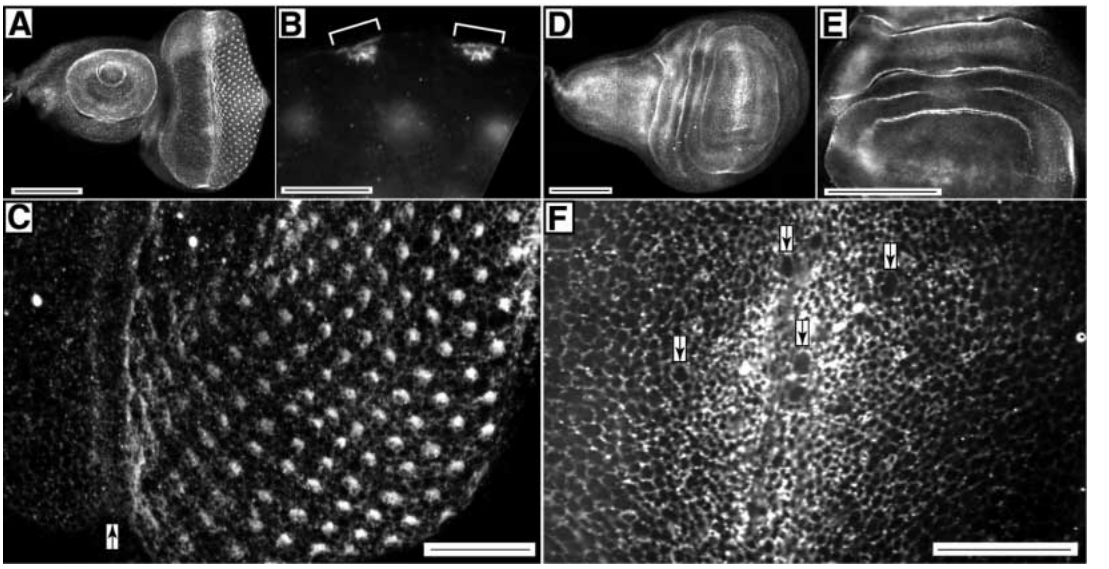

Fig. 4. β_H is apically restricted in 3rd instar imaginal discs and concentrated in ommatidial preclusters. All staining was with mAb 5.73. (A,C,D,F) Focal planes near the apical surface; (B,E) focal planes that section along the apical/basal axes of the epithelia. (A) Whole eye-antennal disc; (B) staining at the edge of an eye disc showing the prominent apical concentration of β_H in the two preclusters present in this optical section (bracketed); (C) part of the apical surface of an eye disc. The arrow indicates the position of the morphogenetic furrow; (D) whole wing disc; (E) staining in the hinge region of a wing disc where the epithelium folds back and forth. β_H is apically localized; (F) part of the apical surface in the wing pouch region of a wing disc. The arrows indicate dividing cells. β_H staining outlines the cells indicating that it is restricted to the apical ends of the lateral membranes. (A,B,D-F) Conventional micrographs; (C) summation of a confocal Z-series (12 sections, 0.5 μm apart). Scale bars: in A, D and E represent 100 μm; in B represents 10 μm; in C and F represent 25 μm.

Sevenless signaling pathway, we performed an epistasis experiment in which we crossed the constitutively activated sevenless receptor, Sev^{S11} (Basler et al., 1991) into a *karst* mutant background. In a wild-type background, Sev^{S11} produces an excess of R7 cells by virtue of the fact that it is expressed in more than one cell per precluster (Basler et al., 1991). In this experiment, siblings with three phenotypes (karst, S11 and S11+karst) were analyzed. If *karst* is epistatic to Sev^{S11} (i.e. blocking signaling when penetrant), we would expect the mean number of R7s per cluster in S11+karst flies to be lower than the mean in S11 flies. Unfortunately, the wider effects of the *karst* mutation on cell position and rhabdomere morphology prevented us from reliably counting the number of R7-type photoreceptors in S11+karst flies. Nevertheless, the mean number of photoreceptors per ommatidium for the S11+karst flies was not significantly different from the S11 flies (data not shown). This is consistent with the interpretation that Sev^{S11} is epistatic to *karst*, suggesting that β_H is upstream of Sevenless or in a parallel pathway contributing to the ligand interaction.

Expression pattern of β_H in the eye and wing discs

To investigate the origins of the *karst* phenotype, we examined the distribution of β_H protein in both the eye/antennal (hereinafter referred to as the eye disc) and wing imaginal disc epithelia. β_H is present in all cells of both discs where it exhibits an apicolateral localization (Fig. 4). Double staining with *D*E-cadherin indicates that this localization coincides with the adherens junctions (Fig. 5A-F). In the eye disc, there is also a greater concentration of β_H at the adherens junctions in the photoreceptor preclusters (Fig. 5A-C) that coincides with more prominent staining for *D*E-cadherin (Fig. 5A-F). These regions correspond to the type III adherens junctions observed by Takahashi et al. (1996). β_H also colocalizes with α-spectrin (Fig. 5G-L); however, the α-spectrin staining extends into the basolateral region of the cells demonstrating that the β_H distribution is apically restricted within the membrane skeleton. Conventional β-spectrin presumably partners α-spectrin in the basolateral regions.

β_H is found in the terminal web of brush borders

The α-spectrin mutation disrupts the microvillar brush border lining on the apical surface of the cell of the cuprophillic cells of the larval midgut (Lee et al., 1993). This mutation presumably compromises the function of both α_2/β_2 and α_2/β_{H2} spectrins. We therefore examined the midgut brush border for the presence of β_H in wild-type flies and for any discernible effects of the *karst* mutation to see if the specific absence of α_2/β_{H2} spectrin would compromise this structure.

β_H is found beneath the brush border in both adults (Fig. 6A,B) and larvae (Fig. 6C). Since we were concerned about the perdurance of maternal product, we examined the adult midgut for defects in *karst* mutants where maternal contribution is not a problem. Here the brush border is well ordered without any consistent irregularities of the cell surface or variations in microvillar length (data not shown).

Infertility

karst mutant flies are very infertile precluding the maintenance of viable homozygous *karst* stocks. A few mutant offspring from ♀ *karst*/deficiency × ♂ *karst*/balancer

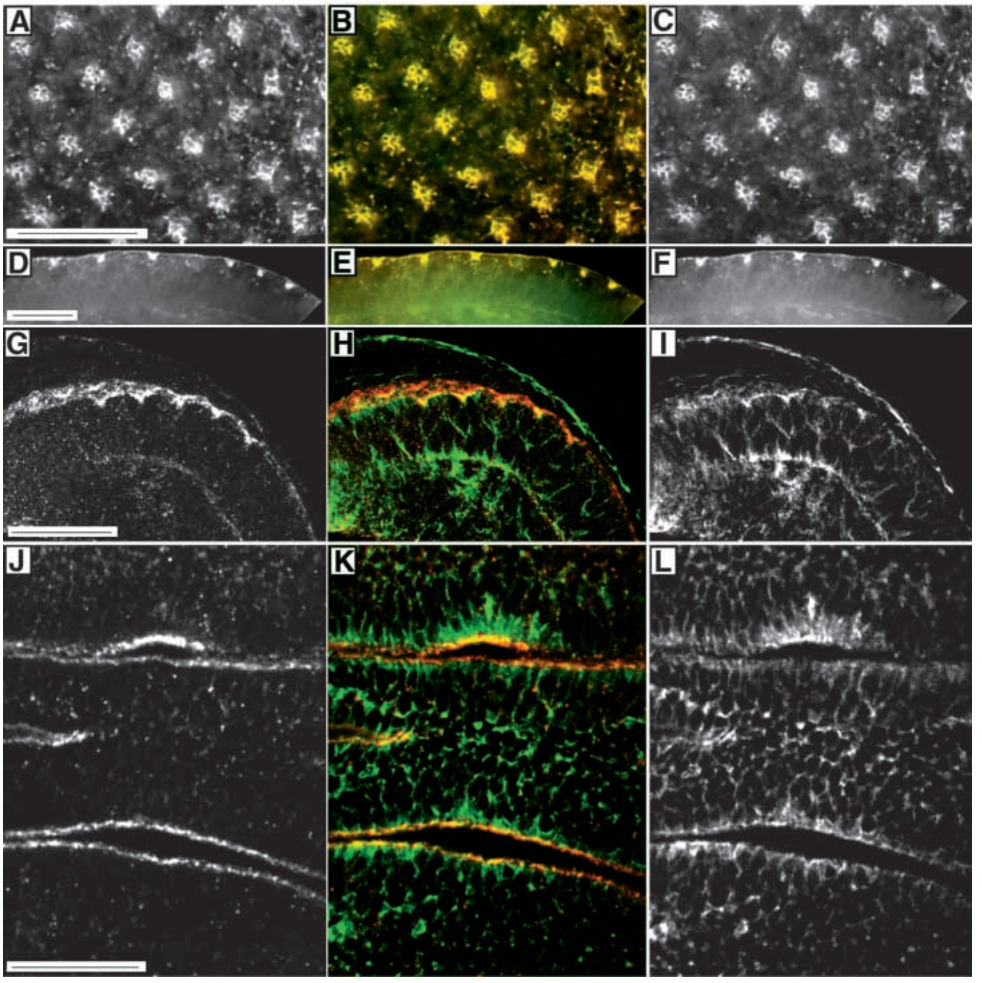

Fig. 5. β_H colocalizes with *D*E-cadherin and apical α-spectrin in imaginal discs. (A-C) En face views of the apical surface of an eye disc behind the morphogenetic furrow; (D-I) sectional view along the apical/basal axis through similar regions; (J-L) apical/basal section through the hinge region of a wing disc. (A,D,G,J) Staining for β_H; (A,D) affinity-purified antibodies from serum #243; (G,J) mAb 5.73. (C,F) Staining for *D*E-cadherin using mAb DCAD2. (I,L) Staining for α-spectrin using serum #905. (B,E,H,K) False-colour composites of the images to the left and right of each panel. β_H staining is indicated by the red channel and *D*E-cadherin or α-spectrin is represented in the green channel. β_H precisely colocalizes with *D*E-cadherin, but only colocalizes with the apical-most extent of the α-spectrin distribution. (A-F) Conventional micrographs; (G-L) confocal micrographs; (G-I) summation of a confocal Z-series (7 sections, 0.2 μm apart). Scale bars in A (for A-C), D (for D-F), G (for G-I) and J (for J-L) all represent 25 μm.

crosses are produced suggesting that, in exceptional cases, individuals may develop in the complete absence of β_H. α-spectrin has been shown to be important for oogenesis both in the follicle cells (Deng et al., 1995; Lee et al., 1997) and in the germline (de Cuevas et al., 1996). Staining of ovaries for β_H reveals that it is primarily concentrated at the apical ends of the somatic follicle cells (Lee et al., 1997; A. E. J. and G. H. T., unpublished data). We stained fixed *karst* mutant egg chambers with rhodamine phalloidin, but this did not reveal any conspicuous defects in the actin cytoskeleton (data not shown).

DISCUSSION

The *karst* phenotype

In order to elucidate further the roles of the spectrin membrane skeleton in development and cell polarity, we have isolated mutations in the gene encoding the protein β_{Heavy}-spectrin (β_H). The primary phenotype is that of larval lethality, variably distributed among the instars; however, small numbers of adults eclose. These adults have visible defects in tissues of epithelial origin; most conspicuously, the eyes are roughened, the wings are curved and the trachea leak haemolymph. β_H is

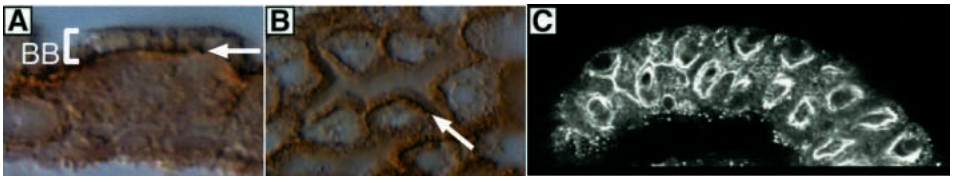

Fig. 6. β_H is a terminal web protein in both the adult and larval midgut. (A) Cross section of cell in the adult thoracic midgut showing prominent staining (arrow) immediately underneath the brush border (BB). (B) Glancing section parallel to the lumenal wall of the adult thoracic midgut, again showing prominent β_H staining underneath the brush borders of several cells (e.g. arrow). (C) Confocal micrograph of the part of the larval midgut where the cuprophilic cells form elaborate saucer-shaped invaginations of their apical surface. These invaginations have a well-developed brush border (Filshie et al., 1971) where β_H is again seen to be in the underlying terminal web. Immunohistochemical (A,B) and immunofluorescent (C) staining for β_H was with the polyclonal antiserum #243 (Materials and Methods).

thus essential for the normal development of the fly. This phenotype probably represents a complete loss of zygotic β_H function since two of our alleles produce no detectable β_H protein and we know that maternal product is not detectable by the third larval instar. All these visible phenotypes exhibit variable expressivity and some are weakly penetrant. Based on our phenotypic analysis, we propose a model whereby ankyrin-independent targeting of β_H to the adherens junction is necessary for juxtacrine Sevenless signaling via its contribution to cadherin-mediated adhesion.

β_H colocalizes with *D*E-cadherin in a membrane skeleton subdomain

The apical subcellular distribution of β_H in both the wing and eye imaginal discs colocalizes with *D*E-cadherin at the adherens junction (Fig. 5), as it does in embryonic epithelia (Thomas and Kiehart, 1994; Uemura et al., 1996; Wodarz et al., 1995). This association appears intimate: in regions of the eye disc where *D*E-cadherin is more abundant (Takahashi et al., 1996), β_H is also more prominent (Fig. 5).

The mutual exclusivity between β_H and the conventional β-spectrin isoform is the norm and may be important for cell polarization (Drubin and Nelson, 1996). While β_H is localized to the adherens junction in imaginal disc epithelia, α-spectrin (presumably partnered by β-spectrin) extends into the basolateral domain (Fig. 5). This is consistent with the apical restriction of β_H in other epithelia (Thomas and Kiehart, 1994; Uemura et al., 1996; Wodarz et al., 1995; de Cuevas et al., 1996; A. E. J. and G. H. T., unpublished observations) and the consistent restriction of β-spectrin to the basolateral membrane (de Cuevas et al., 1996). To establish such a situation, different proteins must recruit the different spectrins to each domain. In the fly, β-spectrin is recruited to the membrane by ankyrin (Dubreuil et al., 1996), while β_H does not colocalize with ankyrin (Lee et al., 1997) and has no conserved ankyrin-binding site (Thomas et al., 1997), suggesting that its interaction with the membrane is not ankyrin dependent. Binding to ankyrin could thus be used to specifically recruit β-spectrin to the basolateral membrane. Presumably the reciprocal situation with some as yet unidentified receptor for β_H results in its apical restriction. This mutually exclusive targeting makes it unlikely that the variable nature of the *karst* mutation is due to partial redundancy of the two β-isoforms.

Disruption of the β_H membrane skeleton may decrease cell-cell adhesion

We propose that the loss of R7 seen in the *karst* mutant eyes is indicative of a reduction in cell adhesion. The commitment of the R7 precursor (pre-R7) to a photoreceptor cell fate requires that the membrane-bound ligand encoded by the *bride of sevenless* gene (BOSS) in R8 must directly contact the *sevenless* receptor (SEV) on the surface of pre-R7 (see Freeman, 1997 for review), and this interaction must sustain a signal for some time to cause this cell fate decision (Bowtell et al., 1988; Mullins and Rubin, 1991). A subpopulation of SEV is seen to concentrate at the adherens junctions specifically in regions in contact with R8 (Tomlinson et al., 1987); however, the bulk of both BOSS and SEV are more apically restricted (Krämer et al., 1991; Tomlinson et al., 1987). If cell adhesion is decreased at the adherens junction, two hypotheses could account for the loss of R7 in *karst* mutant eyes. First, a reduction in BOSS-SEV encounters might cause signaling to drop below the threshold required to trigger R7 commitment. Second, pre-R7 or R8 might move out of position preventing contact and thus signaling. In either case, it seems reasonable to expect that the phenotype would be variable as we see in *karst* mutant eyes.

Two further aspects of the phenotype are consistent with a reduction in cell-cell adhesion. The first is the aberrant arrangement of photoreceptors in *karst* mutant ommatidia. We can readily identify enough properly rotated, trapezoidal ommatidia to indicate that this is probably not a patterning defect. Loosened cell adhesion could readily explain why the cells do not hold their correct relative positions. The second is the leakage of haemolymph from the abdominal spiracles (Fig. 2F). A lack of tracheal integrity might arise because the cells adhere less well to one another. Indeed, we have observed that dissection to remove the gut of 3rd instar larvae is considerably easier in *karst* mutant individuals than their heterozygous siblings, because the trachea are more easily disrupted. Alternatively, the appropriate adhesive contacts may develop incorrectly during pupation leaving gaps in the network.

Spectrins, cell adhesion and signaling

Spectrins can bind directly or indirectly to a number of cell adhesion molecules (Bennett and Gilligan, 1993) suggesting a direct mechanism by which defects in β_H might perturb adhesion, cell-cell contacts and signaling. Here we have shown that the α/β_H-spectrin membrane skeleton is closely associated with cadherin-based adhesion complexes. Existing data indicate that *Drosophila* α/β spectrin is recruited to other cell adhesion complexes (Dubreuil et al., 1996). Such multiple contributions support the observation that disruption of both the α/β-spectrin and α/β_H-spectrin membrane skeletons in α-spectrin mutants has a much more dramatic effect on cell contact (Lee et al., 1993, 1997) than the selective disruption of the α/β_H-spectrin network in *karst* mutants.

A growing body of evidence indicates that tight cadherin-mediated cell-cell adhesion is established *via* intermediate levels of adhesion, involving the clustering of cadherin dimers (Breiher et al., 1996; Gumbiner, 1996; Shapiro et al., 1995), their assembly into higher order structures and the subsequent clustering of such ‘spot adherens junctions’ (Grawe et al., 1996; Tepass and Hartenstein, 1994) or ‘puncta’ (Adams et al., 1996) to establish a mature adherens junction. The actin cytoskeleton is clearly involved in this process (Gumbiner, 1996). The role of long-range and short-range actin crosslinking molecules such as α-actinin and α/β_H-spectrin in such structures is unclear; however, they might serve to increase the density of cadherin molecules associated with F-actin thus strengthening adhesion. The loss of one such crosslinking molecule might only cause a partial reduction in cell adhesion. E-cadherin can be isolated in a complex along with β-spectrin (Nelson et al., 1990); however, the significance of this result is not clear (McCrea and Gumbiner, 1991). More recently a direct association between spectrin and α-catenin has been described (Lombardo et al., 1994; Roe et al., 1996) so a close association between the spectrin membrane skeleton and cadherin cell adhesion complexes seems probable.

We have demonstrated that β_H and *D*E-cadherin colocalize at light microscopic resolution; however, the precise distribution of β_H in ommatidial preclusters may extend to the apico-lateral

margins of the cells above the adherens junction or to form a terminal web-like structure underneath the apical microvillar tufts of the precluster cells (e.g. Krämer et al., 1991). These possibilities suggest two further hypotheses for the role of β_H in Sevenless signaling. First, one or more of the signaling components could bind to the β_H membrane skeleton and the disruption of this association might affect the function or polarization of such components. Second, the role of these microvillar tufts, if any, in signaling remains unknown despite the observation that this is where the bulk of both BOSS and SEV is to be found (Krämer et al., 1991; Tomlinson et al., 1987). However, if they are in some way dependent on α/β_H crosslinking of supporting actin microfilaments, the *karst* mutation might compromise signaling by disrupting this structure. It should also be noted that there remains the formal possibility that β_H is in some way required uniquely in photoreceptor R7 for cell viability. However, there is no suggestion in our existing data that β_H is in any way expressed at different times or levels in the R7 cell compared to the other photoreceptor precursors.

Concluding remarks

It is interesting that we see no apparent effect on some tissues that exhibit prominent β_H expression in the developing organism. Neither the morphology of the musculature nor of the intestinal brush borders appear significantly affected by the *karst* mutation. However, we have not examined the musculature for more subtle defects nor have we subjected it to electrophysiological, mechanical or endurance testing, nor have we performed exhaustive functional tests on either the larval or adult intestinal brush border where β_H is found in the terminal web. During the development of a brush border, the microvilli emerge before a terminal web is visible (Fath and Burgess, 1995), so it may not be surprising that β_H is not necessary for the assembly of microvilli.

McKeown et al. (1998) have recently characterized mutations in the homologous gene in *Caenorhabditis elegans*, *sma-1*. *The sma-1* phenotype is pleiotropic and similar to *karst* insofar as *sma-1* individuals are developmentally delayed and exhibit a defect in a morphogenetic process that has been associated with the apical actin cytoskeleton. However, their results are complementary to ours and reveal an additional role for this class of protein. In contrast to *karst*, the primary defect in *sma-1* mutants is a slowing of a contractile event that normally leads to embryonic elongation. We note that β_H in the fly is conspicuously associated with apical contractions during morphogenesis in the embryo (Thomas and Kiehart, 1994); however, we currently have no data that reveals any similar morphogenetic defects in *karst* mutants.

Our results demonstrate that the apical membrane skeleton is a cellular structure that is essential for normal development. However, the *karst* mutant phenotype is clearly complex, reflecting the multiple structural and signaling roles of this protein complex. We view cytoskeletal elements such as β_H as 'molecular scaffolds' that are used to create specialized membrane domains by locating proteins to, or facilitating specific functions in their vicinity. Clearly a complete understanding of these proteins will only come after specific partners and functionalities are assigned to these various domains.

G. H. T. and D. P. K. are grateful to Bill Gelbart for providing temporary laboratory space during part of this work and to members of the Gelbart laboratory for their advice. We also thank Hany Rizkalla for performing the *karst-DER^{Ellipse}* interaction test; Stephanie Paine-Saunders, James Fristrom, Arthur Wohlwill and Jose Bonner for providing strains, John Lee and Dan Branton for supplying α-spectrin antibodies, and Thuy Nguyen and Beat Suter for initially recognizing that *P{PZ}l(3)01318^{01318}* was a candidate insertion into *karst*. We are grateful to Nate Weymouth, Leslee Conrad and Ruth Montague for technical assistance and to Jon Minden and Charles Ettensohn for the use of their confocal microscope. Finally we thank Bryce MacIver, Esther Siegfried, Meg Titus and Vann Bennett for their critical comments on the manuscript. Funding for this research has come from grants to D. P. K. from The Muscular Dystrophy Association and The National Institutes of Health (NIH; GM33830) and to G. H. T. from The American Heart Association (Pennsylvania Affiliate) and the NIH (GM52506).

Note added in proof

A recent article by Dubreuil et al. (*Dev. Biol.* **194**, 1-11) also identifies β_H as a terminal web protein.

REFERENCES

Adams, C. L., Nelson, W. J. and Smith, S. J. (1996). Quantitative analysis of cadherin-catenin-actin reorganization during development of cell-cell adhesion. *J. Cell Biol.* **135**, 1899-1911.

Ashburner, M. (1989) *Drosophila : A Laboratory Manual*. Cold Spring Harbor, NY, USA: Cold Spring Harbor Press.

Baker, N. E. and Rubin, G. E. (1992). *Ellipse* mutations in the *Drosophila* homologue of the EGF receptor affect pattern formation, cell division, and cell death in eye imaginal discs. *Dev. Biol.* **150**, 381-396.

Ballinger, D. G. and Benzer, S. (1989). Targeted gene mutations in *Drosophila*. *Proc. Natl. Acad. Sci. USA* **86**, 9402-9406.

Basler, K., Christen, B. and Hafen, E. (1991). Ligand-independent activation of the sevenless receptor tyrosine kinase changes the fates of cells in the developing *Drosophila* eye. *Cell* **64**, 1069-1081.

Becker, P. S. and Lux, S. E. (1995). Hereditary Spherocytosis and Hereditary Elliptocytosis. In *The Metabolic and Molecular Basis of Inherited Disease* (ed. C. R. Scriver, A. L. Beaudet, W. C. Sly and D. Valle), pp. 3513-3560. New York: McGraw Hill Inc.

Bell Jr., P. B. and Safiejko-Mroczka, B. (1995). Improved methods for preserving macromolecular structures and visualizing them by fluorescence and scanning electron microscopy. *Scanning Microscopy* **9**, 843-860.

Bennett, V. and Gilligan, D. M. (1993). The spectrin-based membrane skeleton and micron-scale organization of the plasma membrane. *Ann. Rev. Cell Biol.* **9**, 27-66.

Boedigheimer, M., Bryant, P. and Laughon, A. (1993). Expanded, a negative regulator of cell proliferation in *Drosophila*, shows homology to the NF2 tumor suppressor. *Mech. Dev.* **44**, 83-84.

Bowtell, D. D. L., Simon, M. A. and Rubin, G. M. (1988). Ommatidia in the developing *Drosophila* eye require and can respond to *sevenless* for only a restricted period. *Cell* **56**, 931-936.

Breiher, W. M., Yap, A. S. and Gumbiner, B. M. (1996). Lateral dimerization is required for the homophilic binding activity of C-cadherin. *J. Cell Biol.* **135**, 487-496.

Byers, T. J., Brandin, E., Lue, R. A., Winograd, E. and Branton, D. (1992). The complete sequence of Drosophila beta-spectrin reveals supra-motifs comprising eight 106-residue segments. *Proc. Natl. Acad. Sci. USA* **89**, 6187-6191.

Byers, T. J., Dubreuil, R., Branton, D., Kiehart, D. P. and Goldstein, L. S. B. (1987). *Drosophila* spectrin. II. Conserved features of the alpha-subunit are revealed by analysis of cDNA clones and fusion proteins. *J. Cell Biol.* **105**, 2103-2110.

Corces, V., Holmgren, R., Freund, R., Morimoto, R. and Meselson, M. (1980). Four heat shock proteins of *Drosophila melanogaster* coded within a 12-kilobase region in chromosome subdivision 67B. *Proc. Natl. Acad. Sci. USA* **77**, 5390-5393.

de Cuevas, M., Lee, J. K. and Spradling, A. C. (1996). α-spectrin is required for germline cell division and differentiation in the *Drosophila* ovary. *Development* **122**, 3959-3968.

Deng, H., Lee, J. K., Goldstein, L. S. B. and Branton, D. (1995). *Drosophila* development requires spectrin network formation. *J. Cell Biol.* **128**, 71-79.

Ding, D., Parkhurst, S. M. and Lipshitz, H. D. (1993). Different genetic requirements for anterior RNA localization revealed by the distribution of Adducin-like transcripts during *Drosophila* oogenesis. *Proc. Natl. Acad. Sci. USA* **90**, 2512-2516.

Drubin, D. G. and Nelson, W. J. (1996). Origins of cell polarity. *Cell* **84**, 335-344.

Dubreuil, R. R., Byers, T. J., Sillman, A. L., Bar-Zvi, D., Goldstein, L. S. B. and Branton, D. (1989). The complete sequence of *Drosophila* alpha-spectrin: conservation of structural domains between alpha-spectrins and alpha-actinin. *J. Cell Biol.* **109**, 2197-2205.

Dubreuil, R. R., Byers, T. J., Stewart, C. T. and Kiehart, D. P. (1990). A β-spectrin isoform from *Drosophila* (β_H) is similar in size to vertebrate dystrophin. *J. Cell Biol.* **111**, 1849-1858.

Dubreuil, R. R., MacVicar, G., Dissanayake, S., Liu, C., Homer, D. and Hortsch, M. (1996). Neuroglian-mediated cell adhesion induces assembly of the membrane skeleton at cell contact sites. *J. Cell Biol.* **133**, 647-655.

Dubreuil, R. R. and Yu, J. (1994). Ankyrin and β-spectrin accumulate independently of α-spectrin in *Drosophila*. *Proc. Natl. Acad. Sci. USA* **91**, 10285-10289.

Fath, K. R. and Burgess, D. R. (1995). Not actin alone. *Curr. Biol.* **5**, 591-593.

Fehon, R. G., Dawson, I. A. and Artavanis-Tsakonas, S. (1993). A *Drosophila* homologue of membrane-skeleton protein 4.1 is associated with septate junctions and is encoded by the *coracle* gene. *Development* **120**, 545-557.

Filshie, D. K., Pulson, D. F. and Waterhouse, D. F. (1971). Ultrastructure of the copper-accumulating region of the *Drosophila* larval midgut. *Tissue and Cell* **3**, 77-102.

Freeman, M. (1997). Cell determination strategies in the *Drosophila* eye. *Development* **124**, 261-270.

Glenney Jr., J. R., Glenney, P. and Weber, K. (1983). The spectrin-related molecule, TW-260/240, cross-links the actin bundles of the microvillus rootlets in the brush borders of intestinal epithelial cells. *J. Cell Biol.* **96**:1491-96

Grawe, F., Wodarz, A., Lee, B., Knust, E. and Skaer, H. (1996). The *Drosophila* genes *crumbs* and *stardust* are involved in the biogenesis of adherens junctions. *Development* **122**, 951-959.

Grigliatti, T. (1986). Mutagenesis. In *Drosophila; a Practical Approach* (ed. D. B. Roberts), pp. 39-58. Washington DC: IRL Press

Gumbiner, B. (1996). Cell adhesion; the molecular basis of tissue architecture and morphogenesis. *Cell* **84**, 345-357.

Karpen, G. H. and Spradling, A. C. (1992). Analysis of subtelomeric heterochromatin in the *Drosophila* minichromosome DP1187 by single-P-element insertional mutagenesis. *Genetics* **132**, 737-753.

Kiehart, D. P., Montague, R. A., Rickoll, W. L., Foard, D. and Thomas, G. H. (1994). High-resolution microscopic methods for the analysis of cellular movements in *Drosophila* embryos. *Meth. Cell Biol.* **44**, 507-532.

Krämer, H., Cagan, R. L. and Zipursky, S. L. (1991). Interaction of *bride of sevenless* membrane-bound ligand and the *sevenless* tyrosine-kinase receptor. *Nature* **352**, 207-212.

Lambert, S. and Bennett, V. (1993). Postmitotic expression of ankyrinR and beta R-spectrin in discrete neuronal populations of the rat brain. *J. Neurosci.* **13**, 3725-3735.

Lazarides, E., Nelson, W. J. and Kasamatsu, T. (1984). Segregation of two spectrin forms in the chicken optic system: a mechanism for establishing restricted membrane-cytoskeletal domains in neurons. *Cell* **36**, 269-278

Lee, J., Dubreuil, R., Branton, D. and Goldstein, L. (1996). Identification and phenotypic analysis of β-spectrin mutations. *Program and Abstracts. 37th Annual Drosophila Research Conference, San Diego*

Lee, J. K., Brandin, E., Branton, D. and Goldstein, L. S. B. (1997). α-spectrin is required for ovarian follicle monolayer integrity in *Drosophila melanogaster*. *Development* **124**, 353-362.

Lee, J. K., Coyne, R. S., Dubreuil, R. R., Goldstein, L. S. B. and Branton, D. (1993). Cell shape and interaction defects in α-spectrin mutants of *Drosophila melanogaster*. *J. Cell Biol.* **123**, 1797-1809.

Lombardo, C. R., Rimm, D. L., Koslov, E. and Morrow, J. S. (1994). Human recombinant α-catenin binds to spectrin. *Mol. Biol. Cell* **5s**, 47a.

Luna, E. J. and Hitt, A. L. (1992). Cytoskeleton-plasma membrane interactions. *Science* **258**, 955-964.

McCrea, P. D. and Gumbiner, B. M. (1991). Purification of a 92-kDa cytoplasmic protein tightly associated with the cell-cell adhesion molecule E-cadherin (uvomorulin). *J. Biol. Chem.* **266**, 4514-4520.

McKeown, C., Pratis, V. and Austin, J. (1998) The *sma-1* gene encodes a β_{Heavy}-spectrin required for *C. elegans* morphogenesis. *Development* **125**, 2087-2098.

McLean, I. W. and Nakane, P. K. (1974). Periodate-lysine-paraformaldehyde fixative; a new fixative for immunoelectron microscopy. *J. Histochem. Cytochem.* **22**, 1077-1108.

Müller, H.-A. J. and Wieschaus, E. (1996). *armadillo*, *bazooka*, and *stardust* are critical for early stages in formation of the zonula adherens and maintenance of the polarized blastoderm epithelium in *Drosophila*. *J. Cell Biol.* **134**, 149-163.

Mullins, M. C. and Rubin, G. M. (1991). Isolation of temperature-sensitive mutations of the tyrosine kinase receptor *sevenless* (*sev)* in *Drosophila* and their use in determining its time of action. *Proc. Natl. Acad. Sci. USA* **88**, 9387-9391.

Musacchio, A., Gibson, T., Rice, P., Thompson, J. and Saraste, M. (1993). The PH domain: a common piece in the structural patchwork of signaling proteins. *Trends Biochem. Sci.* **18**, 343-348.

Musacchio, A., Wilmanns, M. and Saraste, M. (1994). Structure and function of the SH3 domain. *Prog. Biophys. Mol. Biol.* **61**, 283-297.

Nelson, W. J. (1992). Regulation of cell surface polarity from bacteria to mammals. *Science* **258**, 948-955.

Nelson, W. J., Shore, E. M., Wang, A. Z. and Hammerton, R. W. (1990). Identification of a membrane-cytoskeletal complex containing the cell adhesion molecule uvomorulin (E-cadherin), ankyrin, and fodrin in Mandin-Darby canine kidney epithelial cells. *J. Cell Biol.* **110**, 349-357.

Oda, H., Uemura, T., Harada, Y., Iwai, Y. and Takeichi, M. (1994). A *Drosophila* homologue of cadherin associated with armadillo and essential for embryonic cell-cell adhesion. *Dev. Biol.* **165**, 716-726.

Paine-Saunders, S. (1989). *Drosophila IMP-E2*: the characterization of a gene product expressed during imaginal disc morphogenesis. *Ph.D. Thesis, University of California, Berkeley*

Pesacreta, T. C., Byers, T. J., Dubreuil, R., Kiehart, D. P. and Branton, D. (1989). *Drosophila* spectrin: the membrane skeleton during embryogenesis. *J. Cell Biol.* **108**, 1697-1709.

Riederer, B. M., Zagon, I. S. and Goodman, S. R. (1986). Brain spectrin (240/235) and brain spectrin (240/235E): two distinct spectrin subtypes with different locations within mammalian neural cells. *J. Cell Biol.* **102**, 2088-2097.

Roe, S., Pradhan, D., Koslov, E. R., Morrow, J. S. and Rimm, D. L. (1996). Reduced Binding of mutant α-catenin to spectrin in clone A cells is associated with a non-adhesive phenotype. *Mol. Biol. Cell* **7s**, 285a.

Shapiro, L., Mannon, A. M., Kwong, P. D., Thompson, A., Lehmann, M. S., Grübel, G., Legrand, J.-F., Als-Neilsen, J., Colman, D. R. and Hendrickson, W. A. (1995). Structural basis of cell-cell adhesion by cadherins. *Nature* **374**, 327-337.

Takahashi, F., Endo, S., Kojima, T. and Saigo, K. (1996). Regulation of cell-cell contacts in developing *Drosophila* eyes by *Dsrc41*, a new, close relative of vertebrate c-*src*. *Genes Dev.* **10**, 1645-1656.

Tepass, U. and Hartenstein, V. (1994). The development of cellular junctions in the *Drosophila* embryo. *Dev. Biol.* **161**, 563-596.

Thomas, G. H. and Kiehart, D. P. (1994). β_{Heavy}-spectrin has a restricted tissue and subcellular distribution during *Drosophila* embryogenesis. *Development* **120**, 2039-2050.

Thomas, G. H., Newbern, E. C., Korte, C. C., Bales, M. A., Muse, S. V., Clark, A. G. and Kiehart, D. P. (1997). Intragenic duplication and divergence in the spectrin superfamily of proteins. *Mol. Biol. Evol.* **14**, 1285-1295.

Tomlinson, A., Bowtell, D. D. L., Hafen, E. and Rubin, G. M. (1987). Localization of the *sevenless* protein, a putative receptor for positional information in the eye imaginal disc of *Drosophila*. *Cell* **51**, 143-150.

Uemura, T., Oda, H., Kraut, R., Hayashi, S., Kataoka, Y. and Takeichi, M. (1996). Zygotic DE-cadherin expression is required for processes of dynamic epithelial cell rearrangement in the *Drosophila* embryo. *Genes Dev.* **10**, 659-671.

Van Vactor, D. L., Cagan, R. L., Krämer, G. and Zipursky, S. L. (1991). Induction in the developing compound eye of *Drosophila*: multiple mechanisms restrict R7 induction to a single retinal precursor cell. *Cell* **67**, 1145-1155.

Wodarz, A., Hinz, U., Engelbert, M. and Knust, E. (1995). Expression of CRUMBS confers apical character on plasma membrane domains of ectodermal epithelia of *Drosophila*. *Cell* **82**, 1-20.

Wohlwill, A. D. and Bonner, J. J. (1991). Genetic analysis of chromosome region 63 of *Drosophila melanogaster*. *Genetics* **128**, 763-775.

Yue, L. and Spradling, A. C. (1992). *hu-li tai shao*, a gene required for ring canal formation during *Drosophila* oogenesis, encodes a homologue of adducin. *Genes Dev.* **6**, 2443-2454.

Zaccai, M. and Lipshitz, H. D. (1996). Differential distributions of two adducin-like protein isoforms in the *Drosophila* ovary and early embryo. *Zygote* **4**, 159-166.